The International Journal of Advanced Manufacturing Technology
https://doi.org/10.1007/s00170-019-03714-1

ORIGINAL ARTICLE

Evolution of physical and mechanical characteristics of deposited composite coatings on A356 mild steel

O. S. I. Fayomi[1,2] · G. A. Oluwadare[3] · O. B. Fakehinde[3] · I. G. Akande[4] · W. Nwachia[1] · U. Oziegbe[1] · A. J. Russell[1]

Received: 5 December 2018 / Accepted: 8 April 2019

Abstract
This research investigated the development of $Zn\text{-}SnO_2/Zn\text{-}Al_2SiO_5$ thin film on A356 mild steel using the electrodeposition technique. The developed coating was attained in 2.0 V for 10 min at a constant current density of 1.5 A/cm^2. The electroplating process was maintained at a constant stirring rate of 250 rpm, temperature of 45 °C, 10 g of SnO_2 was used for the bath while Al_2SiO_5 was varied from 5 to 15 g. The surfaces of coated samples were characterized using a scanning electron microscope (SEM). The effects of 3.56% NaCl on the coated and uncoated sample were examined via the potentiodynamic polarization technique, employing Autolab PGSTAT 101 Metrohm potentiostat with NOVA software of version 2.1.2. The outcome of the experiment revealed that the electrodeposited $Zn\text{-}SnO_2/Zn\text{-}Al_2SiO_5$ exhibits better stability, improved microhardness, excellent microstructural qualities, and outstanding corrosion resistance. The $Zn\text{-}10SnO_2\text{-}15Al_2SiO_5$-coated steel exhibits the lowest corrosion rate of 0.0473 mm/year, representing 99.32% reduction in corrosion rate compared to the uncoated sample. Similarly, a corrosion current density (jcorr) value of 20.5 μA/cm^2 was recorded for the uncoated sample which is much greater than the jcorr of the coated samples. This shows that the coating minimizes the exchange of current within the steel. The hardness value of the $Zn\text{-}10SnO_2\text{-}15Al_2SiO_5$-coated steel was higher than other coated samples and 17.51% higher than the uncoated steel, and this indicates improvement in the mechanical property of the steel.

Keywords Characterization · Coating · Electroplating · Mild steel

1 Introduction

Enhancement of the service life of zinc coating by the addition of SnO_2/Al_2SiO_5 nanoparticles into its bath preparation [1] promotes advantageous physical and mechanical characteristics for several industrial applications. The formation of thin-film barrier layers [2, 3], strong adhesion, high stability against mechanical abrasion and chemical attack, and improved microhardness properties are the unique attributes of nanoparticles inclusion in the reinforcement of mild steel [4].

Zinc coatings incorporated with nano had been enlisted as one of the main coating methods used for the protection of mild steel as a result of their cost-effectiveness and unmatchable improvement on the electrochemical and structural properties of mild steel [5]. Their application in manufacturing industries as a protective coating for large quantities of metal products and other fabricated ferrous metallic parts are enormous. Although, nanoparticle composite coatings have been discovered to improved physicochemical and structural properties of mild steel by providing a continuous barrier. However, any imperfection along its surface would inevitably serve as the starting and concentration point for deterioration, if the control is not accelerated [6–8].

During coating process, agitation of the coating bath suspends the particles in the bath and also aids the mass transportation of the particles from the anode to the cathode. The agitation must be moderate so as prevent the movement of the electrodes which could lead to the alteration of charge

✉ O. S. I. Fayomi
ojo.fayomi@covenantuniversity.edu.ng

1 Department of Mechanical Engineering, Covenant University, Ota P.M.B. 1023, Nigeria

2 Department of Chemical, Metallurgical and Materials Engineering, Tshwane University of Technology, Pretoria, South Africa

3 Department of Mechanical and Biomedical Engineering, Bells University of Technology, Ota, Nigeria

4 Department of Mechanical Engineering, University of Ibadan, Ibadan, Oyo State, Nigeria

Published online: 25 April 2019

Table 1 Bath compositions of alloy co-deposition–based matrixes

Composition	Mass concentration
$ZnSO_4$	70 g/L
SnO_2	10 g/L
Al_2SiO_5	5–15 g/L
Glycerin	5 g/L
Boric acid	5 g/L
Thiourea	5 g/L
Sodium sulfate	5 g/L
Potassium sulfate	5 g/L
Operating conditions	2.0 V
Cell voltage	
pH	4.5
Time	10 (min)
Current intensity	1.5 (A/cm^2)

region and consequently altering the quality of particle deposits on the metal [9]. The particulate content in the coating bath and the properties incorporated in the composite deposits are functions of the shape, size, type of particle, and plating bath conditions such as pH, stirring rate, and temperature [10–12]. In the process of deposition, the zinc anode loses electron while the steel gain electrons.

Marine corrosion takes place with parts of piping and equipment that are used in saline water. Degradation of mild steel occurs as a result of constant or occasional exposure of components to seawater. Ships, pipelines, and maritime structures are well-known cases of systems that encounter marine corrosion. In view of this, 3.65% NaCl was simulated and this represents the marine or saline environment. This present research brings new insight into the physical and mechanical performance of mild steel coated with Zn-SnO_2/Zn-SnO_2-Al_2SiO_5 nanoparticles for various industrial applications.

2 Experimental procedures

2.1 Material preparation

The base metal used in this research is rectangular A356 series mild steel plate whose percentage chemical composition is C, 0.15; Mn, 0.45; Si, 0.18; P, 0.01; Al, 0.005; S, 0.031; Ni, 0.008; and Fe, 99.166. Mild steel of dimension (50 mm × 30 mm × 2 mm) and zinc sheets of (90 mm × 50 mm × 10 mm) were prepared. The cathode was mild steel coupons and the anode was the commercially available pure zinc (99.99%). Mild steel was polished with different grades of emery papers. The mild steel sample was made active by dipping into a prepared 10% HCl solution for 5 s, and further rinsed in deionized water of room temperature.

2.2 Bath formulation and deposition of Zn-SnO_2/Zn-SnO_2-Al_2SiO_5

The coating solution was prepared with analar grade of chemicals and deionized water at room temperature before coating. The bath formulation shown in Table 1 was prepared for the coating process and continuously stirred at 250 rpm and 45 °C constant heating although the deposition period, so as to obtain stabilized suspension that is devoid of particles' agglomeration. Avoiding agglomeration of particles promotes the mobility electrophoresis of the coating solution [13].

In the deposition process, the mild steel being the cathode was placed equidistance from two zinc plates and connected to the negative terminal of the rectifier in the bath as shown in Fig. 1. The zinc anodes were connected to the positive terminal of the rectifier [14, 15]. The pH used was 4.5; other plating parameters such as voltage, current density, and time were kept at 2.0 V, 1.5 A/cm^2, and 10 min, respectively, as

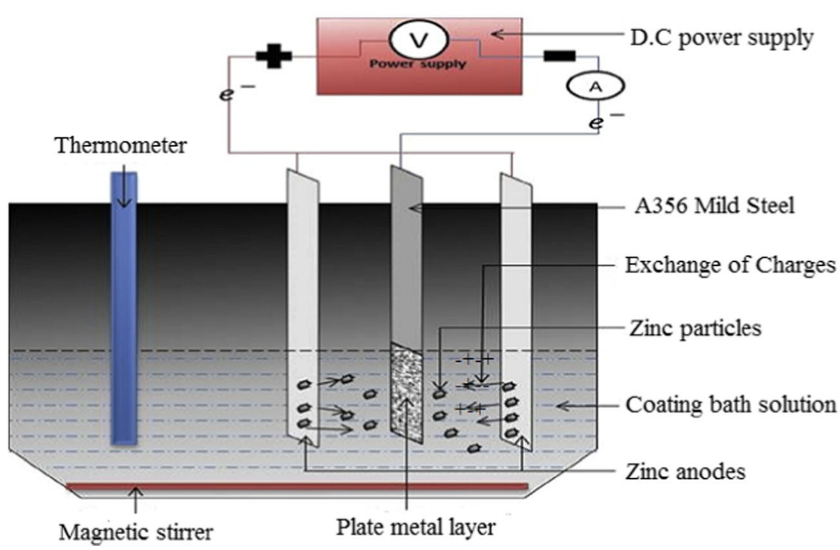

Fig. 1 Schematic diagram of a co-deposition system

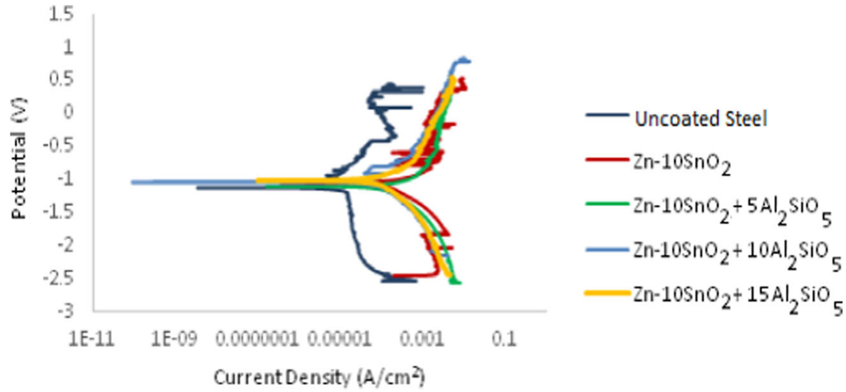

Fig. 2 Potentiodynamic polarization curves of $Zn-SnO_2$/$Zn-SnO_2-Al_2SiO_5$-coated and uncoated samples

presented in Table 1. The coatings of the samples were strategically done with reference to ASTM A53/A53M and A153.

2.3 Material characterization and structural test

The morphology and adhesion of $Zn-SnO_2$/$Zn-SnO_2-Al_2SiO_5$ on the surface mild were examined using a scanning electron microscope (SEM). The electrochemical behavior was investigated with the use of the standard three-electrode cell. Potentiodynamic measurements (− 1.5 V/Eocp to 1.5 V/SSCE, 0.005 mV/s) were performed after 60 min of stabilization of open circuit potential in a 3.65% NaCl solution. Brinell technique was used to characterize the microhardness properties of the coated and uncoated samples. This was done in accordance with our previous work Ref. [16].

3 Results and discussion

3.1 Electrochemical test

Potentiodynamic polarization measurements were performed to evaluate the corrosion defense of the embedded nanoparticles. Figure 2 shows the plots of the potentiodynamic curves of $Zn-SnO_2$/$Zn-SnO_2-Al_2SiO_5$-coated and uncoated specimens. The values of corrosion current density of the coated samples were found to be smaller than those of the uncoated. This attests that the coating barred the active sites of the steel preventing transfer of current. The coatings were able to form inhibition barriers, therefore limiting the cathodic evolution and anodic metal dissolution reactions of the mild steel [17–20]. $Zn-SnO_2$/$Zn-SnO_2-Al_2SiO_5$ composite coatings are mixed inhibitors but less negative values of the Ecorr of the coated samples with respect to the control imply that the coatings performed predominantly as anodic inhibitors.

As indicated in Table 2, the corrosion rate of the uncoated steel was 2.59 mm/year; the $Zn-10SnO_2$-coated steel has the highest corrosion rate among the coated samples with a value of 1.134 mm/year. $Zn-10SnO_2-15Al_2SiO_5$-coated sample possesses a lower corrosion rate value of 0.0473 mm/year. The low corrosion rate could be attributable to the quality and tenacity of the passive film generated by $Zn-10SnO_2-15Al_2SiO_5$ on the surface of the coated steel or elemental stability of the sample [21].

3.2 Microstructure analysis

The morphology of $Zn-SnO_2$/$Zn-SnO_2-Al_2SiO_5$-coated steel was exposed in the SEM micrographs shown in Fig. 3. Significantly, the crystallites of the deposits are homogenously distributed on the steel samples, signifying regenerated materials with better corrosion and mechanical properties [22]. The SEM micrographs present nanocomposite structure along the boundary as a result of the alliance of notable crystallite of $SnO_2-SnO_2-Al_2SiO_5$ nanoparticulates. More so, two expected phases can be seen in the SEM micrographs in Fig. 2, indicating the embodiment of the SnO_2 and Al_2SiO_5 in the zinc interface, displaying immeasurable and embellished nodular structures on the coating network. This was found to grow with the addition in the mass concentration

Table 2 Potentiodynamic polarization data of $Zn-SnO_2$/$Zn-SnO_2-Al_2SiO_5$ deposition

Samples	jcorr (μA/cm^2)	RP (Ω)	Ecorr (V)	Corrosion rate (mm/yr)	Percentage reduction of corrosion rate (%)
Uncoated	20.5	199.0	− 1.2124	2.59	0
$Zn-10SnO_2$	11.5	389.9	− 1.0469	1.134	56.22
$Zn-10SnO_2-5Al_2SiO_5$	9.15	297.0	− 1.0980	0.965	62.74
$Zn-10SnO_2-10Al_2SiO_5$	6.32	893.3	− 1.0329	0.0734	97.17
$Zn-10SnO_2-15Al_2SiO_5$	4.07	1175.8	− 1.0058	0.0473	99.32

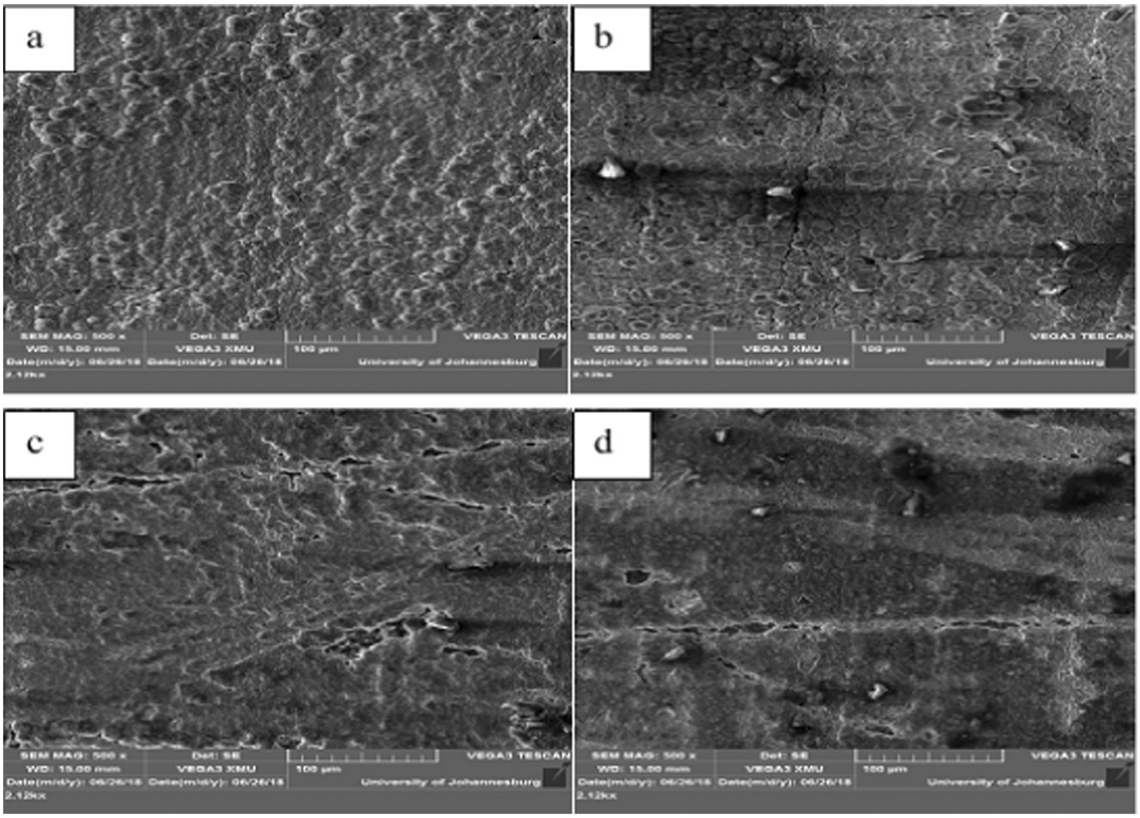

Fig. 3 SEM micrographs of **a** Zn-10SnO_2-, **b** Zn-10SnO_2-5Al_2SiO_5-, **c** Zn-10SnO_2-10Al_2SiO_5-, and **d** Zn-10SnO_2-15Al_2SiO_5-coated steel

of Al_2SiO_5. It is worthy of note that the corresponding and synergistic effect of SnO_2 and Al_2SiO_5 nanoparticles strengthens the coating system and further provided refined and attractive morphology for the coated samples. This was indeed suspected considering the pathway of nucleation, which originated from the zinc metal as a load carrier; the diffusion of the particulates affects the nucleation domains and consequently improving the developed nanocomposites [23].

Moreover, it is vital to intimate that the scanty change in microstructure of Fig. 3c and d could be traceable to the increment in the mass concentration of Al_2SiO_5 nanoparticulates blended into the nanocomposite coatings resulting to improved precipitation and enhanced coating. One can, consequently, infer that the hardness of the composite coatings increased with the incorporation of Al_2SiO_5 particles in the coating. This is in accordance with the conclusion of other authors [24, 25].

3.3 Microhardness analysis

The microhardness results obtained for the Zn-SnO_2/Zn-SnO_2-Al_2SiO_5 deposit are presented in Fig. 4. Upon observation, Zn-10SnO_2-15Al_2SiO_5 gave the highest hardness reading. Using the Brinell hardness value, the substrate material hardness rose from 177 BHN to 208 BHN after composite deposition. This is in accordance with ASTM A-370 and A833. Generally, the hardness value for all the samples with differing additives shows an increase. This furthermore implies that the improvement in hardness could be attributed to the creation of an adhesive mechanism of the composite coating on the substrate sample. Also, microhardness of electrodeposited coatings is dependent on operating factors such as bath ingredients and other processing parameters [25, 26].

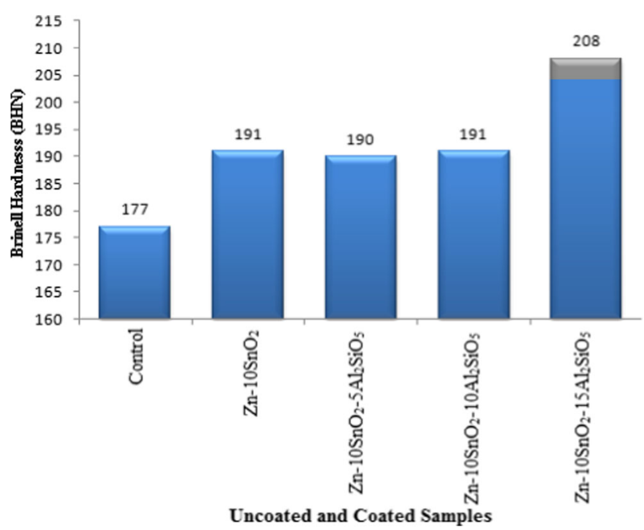

Fig. 4 Brinell microhardness property of Zn-SnO_2/Al_2SiO_5-coated and uncoated mild steel

4 Conclusions

Incorporation of SnO_2/Al_2SiO_5 into Zn composite coating improved the corrosion resistance, with mixed inhibitive characteristics. The Zn-10SnO_2-15Al_2SiO_5-coated steel exhibits the lowest corrosion rate of 0.0473 mm/year, representing 99.32% reduction in corrosion rate compared to the uncoated sample. The SEM micrograph displays excellent morphology of SnO_2-Al_2SiO_5-coated steel. The increase in microhardness from 177 BHN to 208 BHN attests to an improvement in the mechanical properties of the coated steel. The study has presented remarkable insight into the application of nanocomposite firm for corrosion protection and structural enhancing properties.

References

1. Fayomi OSI, Popoola API (2015) Anti-corrosion and tribo-mechanical properties of co-deposited Zn–SnO_2 composite coating. Acta Metall Sin (Engl Lett) 28(4):521–530
2. Lee YS, Heo J, Siah SC, Mailoa JP, Brandt RE, Kim SB, Gordon RG, Buonassisi T (2013) Ultrathin amorphous zinc-tin-oxide buffer layer for enhancing heterojunction interface quality in metal-oxide solar cells. Energy Environ Sci 6(7):2112–2118
3. Inoue T, Osonoe M, Tohda H, Hiramatsu M, Yamamoto Y, Yamanaka A, Nakayama T (1991) Low-temperature epitaxial growth of cerium dioxide layers on (111) silicon substrates. J Appl Phys (12):813–815
4. Toro RG, Malandrino G, Fragalà IL, Lo Nigro R, Losurdo M, Bruno G (2004) Relationship between the nanostructures and the optical properties of CeO_2 thin films. J Phys Chem B 108(42): 16357–16364
5. Aigbodion VS, Fayomi OSI (2016) Anti-corrosion coating of mild steel using ternary Zn-ZnO-Y_2O_3 electro-deposition. Surf Coat Technol 306:448–454
6. Fayomi OSI, Abdulwahab M, Popoola AP, Asuke F (2015) Corrosion resistance of AA6063-type Al-Mg-Si alloy by silicon carbide in sodium chloride solution for marine application. J Mar Sci Appl 14(4):459–462
7. Bankole MT, Abdulkareem AS, Tijani JO, Ochigbo SS, Afolabi AS, Roos WD (2017) Chemical oxygen demand removal from electroplating wastewater by purified and polymer functionalized carbon nanotubes adsorbents. Water Resour Ind 18:33–50
8. Winkler DA, Breedon M, White P, Hughes AE, Sapper ED, Cole I (2016) Using high throughput experimental data and in silicon models to discover alternatives to toxic chromate corrosion inhibitors. Corros Sci 106:229–235
9. Low CT, Wills RG, Walsh FC (2006) Electrodeposition of composite coatings containing nanoparticles in a metal deposit. Surf Coat Technol 12(201(1–2)):371–383
10. Alirezaei S, Monirvaghefi SM, Salehi M, Saatchi A (2007) Wear behavior of Ni–P and Ni–P–Al2O3 electroless coatings. Wear. 262(7–8):978–985
11. Bulasara VK, Thakuria H, Uppaluri R, Purkait MK (2011) Effect of process parameters on electroless plating and nickel-ceramic composite membrane characteristics. Desalination. 268(1–3):195–203
12. Szczygieł B, Turkiewicz A, Serafińczuk J (2008) Surface morphology and structure of Ni–P, Ni–P–ZrO2, Ni–W–P, Ni–W–P–ZrO2 coatings deposited by electroless method. Surf Coat Technol 202(9):1904–1910
13. Daniyan AA, Umoru LE, Fayomi OSI (2018) Structural evolution, optoelectrical and corrosion properties of electrodeposited WO_3 integration on Zn-TiO_2 electrolyte for defence super application. Def Technol 14:396–402
14. Achi SS (2003) Basic principles of coating technology. Shemang Graphics, Zaria, pp 1–2
15. Fayomi OSI, Abdulwahab M (2013) Property's evaluation of ternary surfactant-induced Zn-Ni-Al_2O_3 films on mild steel by electrolytic chemical deposition. J Ovonic Res 5:123–132
16. Dutta A, Saha SK, Adhikari U, Banerjee P, Sukul D (2017) Effect of substitution on corrosion inhibition properties of 2-(substituted phenyl) benzimidazole derivatives on mild steel in 1 M HCl solution: a combined experimental and theoretical approach. Corros Sci 123:256–266
17. Rossrucker L, Samaniego A, Grote JP, Mingers AM, Laska CA, Birbilis N, Frankel GS, Mayrhofer KJ (2015) The pH dependence of magnesium dissolution and hydrogen evolution during anodic polarization. J Electrochem Soc 7:333–339
18. Fayomi OSI, Akande IG, Popoola API (2018) Corrosion protection effect of chitosan on the performance characteristics of A6063 alloy. J Bio-and Tribo-Corrosion 4(4):73
19. Fayomi OSI, Akande IG, Oluwole OO, Daramola D (2018) Effect of water-soluble chitosan on the electrochemical corrosion behaviour of mild steel. Chem Data Collect 17-18:321–326
20. Popoola API, Daniyan AA, Umoru LE, Fayomi OSI (2017) Effect of WO_3 nanoparticles loading on the microstructural, mechanical and corrosion resistance of Zn matrix/TiO_2-WO_3 nanocomposite coatings for marine application. Sci Appl 16:1389–1387
21. Alhawari KS, Omar MZ, Ghazali MJ, Salleh MS, Mohammed MN (2013) Wear properties of A356/Al_2O_3 metal matrix composites produced by semisolid processing. Procedia Eng 68:186–192
22. Oluyori T, Olorunniwo OE, Fayomi OSI, Atanda PO (2017) Performance evaluation effect of Nb_2O_5 particulate on the microstructural, wear and anti-corrosion resistance of Zn–Nb_2O_5 coatings on mild steel for marine application. J Bio-and Tribo-Corrosion 3(4):51
23. Akarapu A (2011) Surface property modification of copper by nanocomposite coating. M.Tech. Thesis. Rourkela, Indian: Department of Metallurgical and Materials Engineering, National Institute of Technology
24. Alhawari KS, Omar MZ, Ghazali MJ, Salleh MS, Mohammed MN (2013) Wear properties of A356/Al_2O_3 metal matrix composites produced by semisolid processing. Procedia Eng 68:186–192
25. Rusu DE, Ispas A, Bund A, Gheorghies C, Carac G (2012) Corrosion tests of nickel coatings prepared from a Watts-type bath. J Coat Technol Res 9(1):87–95
26. Akande IG, Oluwole OO, Fayomi OSI (2018) Optimizing the defensive characteristics of mild steel via the electrodeposition of Zn-Si_3N_4 reinforcing particles. Def Technol. https://doi.org/10.1016/j.dt.2018.11.00